



Synthesis and thermoelectric properties of the $\text{PbSe}_{1-x}\text{Te}_x$ alloys

J.Q. Li*, S.P. Li, Q.B. Wang, L. Wang, F.S. Liu, W.Q. Ao

College of Materials Science and Engineering, Shenzhen University and Shenzhen Key Laboratory of Special Functional Materials, Shenzhen 518060, PR China

ARTICLE INFO

Article history:

Received 19 November 2010

Received in revised form

30 December 2010

Accepted 4 January 2011

Available online 16 January 2011

Keywords:

PbSe thermoelectric materials

Mechanical alloying

SPS sintering

Thermoelectric property

ABSTRACT

The $\text{PbSe}_{1-x}\text{Te}_x$ alloys with $x=0.2, 0.3, 0.5, 0.85$ and 1.0 were prepared by induction melting, ball milling and spark plasma sintering techniques. The thermoelectric properties of the samples were investigated. The XRD analysis indicated that all samples are NaCl-type structure solid solutions $\text{Pb}(\text{Se},\text{Te})$ containing nanograins. Increasing Te content resulted in increasing the lattice parameter a . The thermoelectric measurements show that all samples are n-type semiconductors in temperature range from 300 K to 673 K. The electrical resistivity of the doped sample is much smaller than that of pure PbSe, but comparable to that of PbTe. The absolute Seebeck coefficients for the doped sample $\text{PbSe}_{1-x}\text{Te}_x$ with $x=0.2, 0.3$ and 0.5 range from $150 \mu\text{V}/\text{K}$ at 300 K to $250 \mu\text{V}/\text{K}$ at 673 K, which is much larger than that of pure PbSe ($66\text{--}138 \mu\text{V}/\text{K}$), but smaller than that of PbTe ($230\text{--}310 \mu\text{V}/\text{K}$) in the same experimental conditions. The thermal conductivity for the doped sample $\text{PbSe}_{1-x}\text{Te}_x$ with $x=0.2, 0.3$ and 0.5 range from 0.95 to $0.66 \text{ W}/\text{m K}$, which is much smaller than that of pure PbSe ($2.1\text{--}1.3 \text{ W}/\text{m K}$) or PbTe ($1.4\text{--}1.1 \text{ W}/\text{m K}$). As a result, the figure of merit for the doped sample can be enhanced. The maximum dimensionless figure of merit ZT of 1.15 was obtained in the sample $\text{PbTe}_{0.5}\text{Se}_{0.5}$ at 573 K, more than 50% higher than that of pure PbTe prepared in the same condition.

© 2011 Elsevier B.V. All rights reserved.

1. Introduction

Thermoelectric (TE) materials are capable of realizing the conversion of heat into electricity or electricity into heat. Therefore, thermoelectric devices have attracted extensive interest for several decades due to the potential applications on producing electricity from the waste heat and thermoelectric cooling. The efficiency of the TE materials is determined by the dimensionless figure of merit $ZT = S^2\sigma T/\kappa$, where S, σ, T and κ are the Seebeck coefficient, the electrical conductivity, the absolute temperature and the thermal conductivity, respectively. The effort to improve ZT is to minimize the thermal conductivity and maximizing the power factor $S^2\sigma$.

PbSe and PbTe are two types of candidate thermoelectric materials. PbSe has received comparatively little attention perhaps because of its lower figure-of-merit as comparing with that of PbTe at intermediate temperature [1]. However, PbSe has its advantages relative to PbTe: first, Se is more commonly available and less expensive than Te, and second, the melting point of PbSe is substantially higher, at 1340 K, than PbTe at 1190 K. Recently, more attention was paid to the investigation of PbSe based compounds as thermoelectric materials for cooling and power generation applications. Unuma et al. reported the thermoelectric properties of PbSe compound prepared by pressureless sintering [2]. Substitution of

Sm for Pb in PbSe can enhance its thermoelectric performance [3]. Parker predicted that properly hole-doped bulk PbSe may offer better thermoelectric performance than the PbTe [4]. The lattice thermal conductivity of $\text{PbSeTe}/\text{PbTe}$ quantum dot superlattice has the value of $0.33\text{--}0.4 \text{ W m}^{-1} \text{ K}^{-1}$ at room temperature leading to the ZT value reaching 2.0 at 300 K [5]. The thermoelectric properties of Se-rich $\text{PbSe}_{1-x}\text{Te}_x$ alloys have not been reported so far, so we investigated it in this paper.

2. Experimental

The elements Pb, Te and Se with purity of 99.99% were used as starting materials. The compounds PbSe and PbTe were prepared by high-frequency induction melting in evacuated quartz tubes and then ball milled into the powders with particle size of about tens nm, separately. Subsequently, the mixture powders with compositions of $\text{PbSe}_{1-x}\text{Te}_x$ ($x=0.2, 0.3, 0.5, 0.85$ and 1.0) were prepared by ball milling using the milled PbSe and PbTe powders. The ball milling was carried out in a planetary ball mill (QM-4F, Nanjing University, China) using a hard stainless steel vial and balls, at 200 rpm for 5 h for the pure PbSe and PbTe powders, while at 200 rpm for 14 h for the mixture powders. The weight ratio of balls to powders was kept at about 20:1, and the mill vial was evacuated and then filled with a pure H_2 atmosphere to prevent the powders from oxidation during the milling process. The ball milling of the pure PbSe and PbTe powders firstly can reduce the grain size in the sample and modify the grain boundaries by forming the solid solution during the ball milling and spark plasma sintering of the mixture powder, which should benefit the electrical conductivities of the samples. The sample powders were consolidated by spark plasma sintering (SPS) at 743 K for 5 min under an axial pressure of 32 MPa. The bar specimen with dimensions of $12.0 \text{ mm} \times 5.0 \text{ mm} \times 5.0 \text{ mm}$ was prepared for the electrical properties measurement and the disk specimen with $\phi 12.7 \text{ mm} \times 2.0 \text{ mm}$ for the thermal conductivity measurement.

* Corresponding author. Tel.: +86 755 26538528; fax: +86 755 26538528.
E-mail address: junqinli@szu.edu.cn (J.Q. Li).

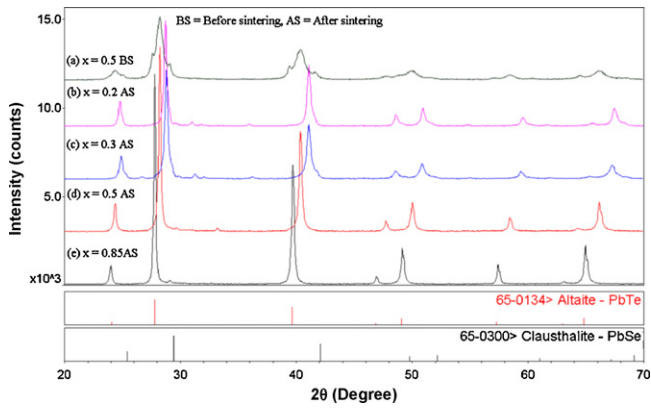


Fig. 1. Powder XRD patterns for the samples $\text{PbTe}_x\text{Se}_{1-x}$ with (a) $x=0.5$ before sintering; (b) $x=0.2$, (c) $x=0.3$, (d) $x=0.5$ and (e) $x=0.85$ after sintering.

The phases in the samples were analyzed by X-ray diffraction using a Bruker D8 Advance SS/18 kW diffractometer with $\text{Cu K}\alpha$ radiation and JADE 5.0 software. The Rietveld refinements of the XRD patterns were performed using Topas 3.0 software. The Seebeck coefficient (S) and electrical conductivity (σ) were evacuated by the apparatus (ZEM-2, Ulvac-Riko, Japan) in a helium atmosphere. The thermal conductivity (κ) was calculated using the equation $\kappa = \lambda C_p d$, where λ is the thermal diffusivity, C_p is the heat capacity, and d is the bulk density of the sample. The thermal diffusivity was measured by a laser flash technique (NETZSCH LFA457) in Ar

atmosphere. The heat capacity was measured by the differential scanning calorimetry. The bulk density of the sample was calculated from the sample's geometry and mass.

3. Results and discussion

3.1. Phase analysis

Fig. 1 shows the powder X-ray diffraction patterns for some representative samples before and after sintering. The XRD pattern for the sample $\text{PbTe}_{0.5}\text{Se}_{0.5}$ before sintering, shown in Fig. 1(a), indicates that the sample consists of PbSe and PbTe , together with the solid solution $\text{Pb}(\text{Se},\text{Te})$. It means that the solid solution $\text{Pb}(\text{Se},\text{Te})$ can partly be formed during ball milling of the PbTe and PbSe mixture powder. The Rietveld refinement using Topas 3.0 software for this sample, shown in Fig. 2(a), indicates that 73.0 wt.% of the solid solution $\text{Pb}(\text{Se},\text{Te})$ can be formed after ball milling the mixture powders at 200 rpm for 14 h. The broad peaks appear in the XRD pattern of the sample before sintering due to the small particle size of the powders and the existence of stress and strain after the ball milling process. Considering the particle size and the strain, the Rietveld refinement results estimated that the sample contained nanocrystallite grains with an average size of 28 nm in the solid solution $\text{Pb}(\text{Se},\text{Te})$. The SEM and the bright-field TEM observations for the PbTe powders prepared by ball milling reported in

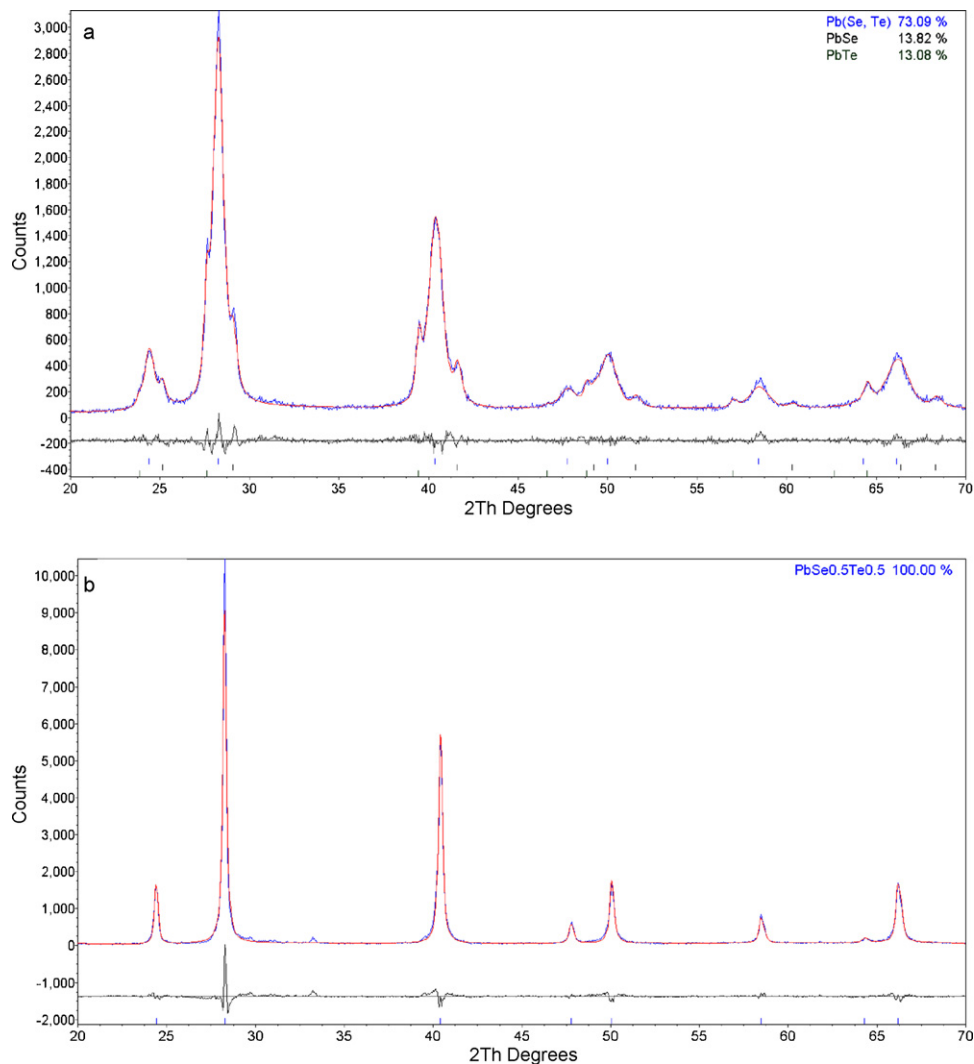


Fig. 2. Rietveld refinement for the XRD patterns of the sample $\text{PbTe}_{0.5}\text{Se}_{0.5}$ (a) before and (b) after SPS sintering.

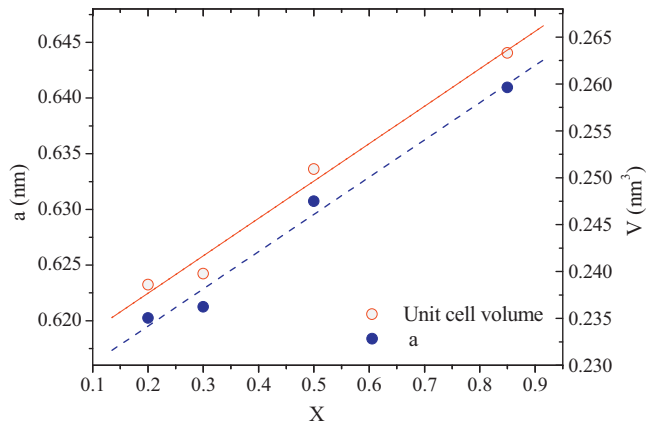


Fig. 3. Compositional dependence of the lattice parameters a and the unit volume $V(c)$ for $\text{PbTe}_x\text{Se}_{1-x}$ solid solution.

Ref. [6] showed that the powders contained nanocrystallite grains and micrometer grains. The XRD peak broadening of the powder is mainly contributed from the nanocrystallite grains. The average grain size of 41 nm of the nanocrystallite grain was determined from the full-width at half-maximum of the XRD peak broadening. Therefore, we believe that the solid solution $\text{Pb}(\text{Se},\text{Te})$ in this work has the similar behavior, which contains some micrometer grains and some nanometer grains with an average size of 28 nm determined from its XRD peak broadening. Fig. 1(b)–(e) shows the XRD patterns for the samples $\text{PbSe}_{1-x}\text{Te}_x$ with $x=0.2, 0.3, 0.5$ and 0.85 after sintering, respectively, which indicates that the samples after sintering formed the NaCl-type structure solid solution $\text{Pb}(\text{Se},\text{Te})$ single phase without any noticeable secondary phase. The Rietveld

refinement results, shown in Fig. 2(b) for the sample $\text{PbTe}_{0.5}\text{Se}_{0.5}$ after sintering as an example, estimated that the average size of the nanocrystallite grains becomes about 50 nm. The formation of the solid solution $\text{Pb}(\text{Se},\text{Te})$ by diffusion of Se and Te between the PbTe and PbSe phases in the mixture powders during ball milling and SPS process can modify the interface between powder particles and benefits to the electrical conductivity. The X-ray diffraction pattern of the samples $\text{PbSe}_{1-x}\text{Te}_x$ after sintering shifts to low 2θ angle as Te content x increases, indicating that the lattice parameter a and the volume of the unit cell of solid solution $\text{Pb}(\text{Se},\text{Te})$ increases as Te content x increases, shown in Fig. 3, due to the substitution of larger Te atom for smaller Se atom in the compound.

3.2. Thermoelectric properties

The temperature dependence of electrical resistivity, Seebeck coefficient, thermal conductivity and dimensionless figure of merit ZT for the samples $\text{PbSe}_{1-x}\text{Te}_x$ with $x=0.2, 0.3, 0.5, 0.85$ and 1.0 is shown in Fig. 4. The temperature dependence of electrical resistivity, Seebeck coefficient for pure PbSe compound prepared by pressureless sintering reported in Ref. [2] and the thermal conductivity for this compound prepared by melting [7] is also given in the figure for comparing. The electrical resistivity of $2.8\text{--}9.5 \times 10^{-5} \Omega\text{m}$, the absolute Seebeck coefficient of $227\text{--}312 \mu\text{V/K}$, the thermal conductivity of $1.4\text{--}1.1 \text{ W/mK}$ and the figure of merit ZT of $0.39\text{--}0.75$ were obtained in the sample PbTe in this work in temperature range from 300K to 673K , which is in good agreement with those of the PbTe prepared by ball milling and SPS process reported in Ref. [6]. The electrical resistivities for all the studied samples except $x=0.85$, shown in Fig. 3(a), increase with increasing temperature, indicating the degenerate semiconductor behavior due to the positive temperature coefficient

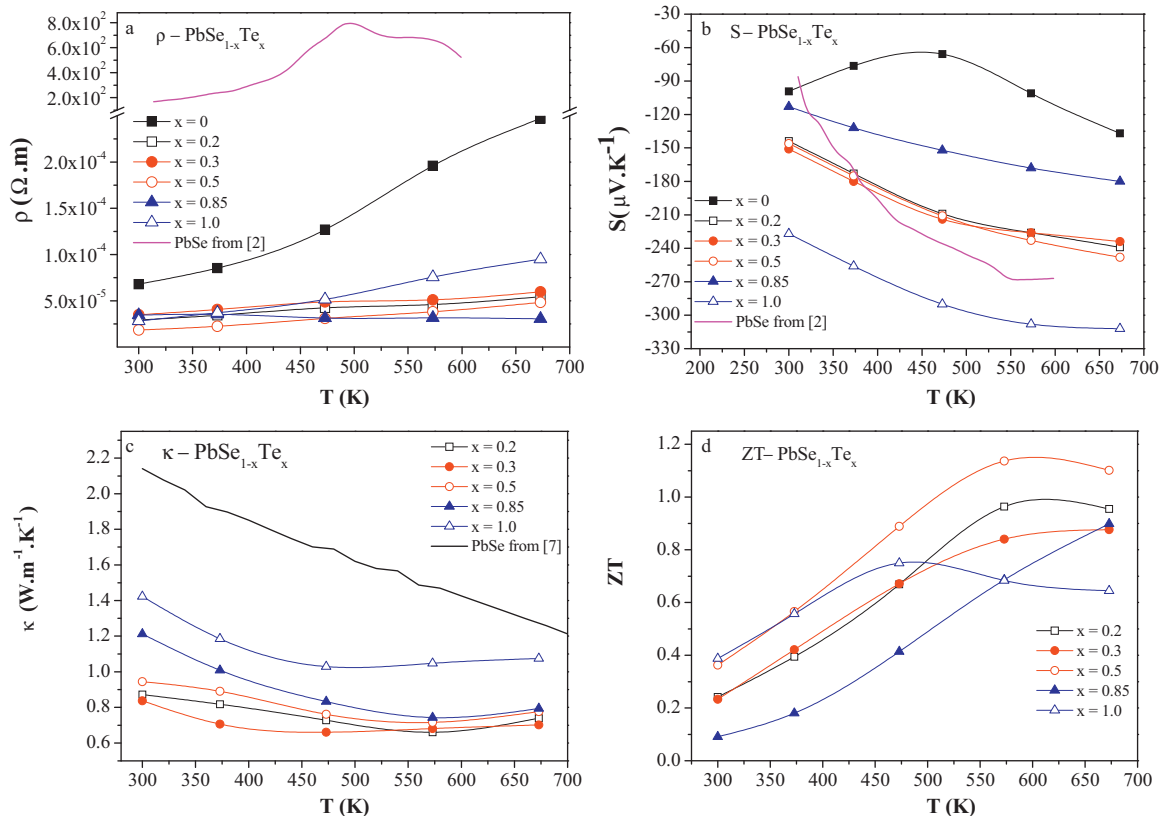


Fig. 4. Temperature dependence of the (a) electrical resistivity ρ , (b) Seebeck coefficient S , (c) thermal conductivity κ and (d) figure of merit ZT for the samples $\text{PbTe}_x\text{Se}_{1-x}$ with $x=0.2, 0.3, 0.5, 0.85$ and 1.0 . The temperature dependence of electrical resistivity, Seebeck coefficient for pure PbSe compound prepared by pressureless sintering reported in Ref. [2] and the thermal conductivity for this compound prepared by melting [7] is also given in the figure for comparing.

cient, resulting from the phonon scattering of charge carriers. For the sample with $x=0.85$, its resistivity reduces slightly with increasing temperature. No systematic trend was found in the variation of the electrical resistivity for $\text{PbSe}_{1-x}\text{Te}_x$ samples with Te content, but electrical resistivities in ternary samples with $x=0.2, 0.3, 0.5$ and 0.85 , below $3.5 \times 10^{-5} \Omega \text{ m}$ at 300 K and $6.0 \times 10^{-5} \Omega \text{ m}$ at 673 K, are lower than those of the binary compound PbTe or PbSe, resulting in the Te doping level. The electrical resistivity for PbSe in this work, between $6.8 \times 10^{-5} \Omega \text{ m}$ at 300 K and $2.5 \times 10^{-4} \Omega \text{ m}$ at 673 K, are much lower than those of pure PbSe compound prepared by pressureless sintering, 167 $\Omega \text{ m}$ at 300 K and 782 $\Omega \text{ m}$ at 473 K, reported in Ref. [2]. The high electrical resistivity in the pressureless sintered sample may be caused by the oxide impurity phase in the grain boundary and the number of the grain boundary [2]. The Te doping level and grain boundary resistance may play important role for reducing electrical resistivity. The modification of the interface between the grains, by the formation of the solid solution $\text{Pb}(\text{Se},\text{Te})$ by diffusion of Se and Te between the PbTe and PbSe phases in the mixture powders during ball milling and SPS process, may be an effective way to reduce the electrical resistivity of the samples.

The Seebeck coefficients of the studied samples, shown in Fig. 4(b), were found to be negative value over the entire temperature range, indicating that the n-type (electron) carriers dominate the thermoelectric transport. The absolute values of Seebeck coefficients $|S|$ of all the samples increase with increasing temperature, which follow the trend of temperature-dependant electrical resistivities. The absolute Seebeck coefficients for the doped sample $\text{PbSe}_{1-x}\text{Te}_x$ with $x=0.2, 0.3$ and 0.5 range from 150 $\mu\text{V/K}$ at 300 K to 250 $\mu\text{V/K}$ at 673 K, which is much larger than that of pure PbSe (66–138 $\mu\text{V/K}$) or the sample with $x=0.85$ (113–180 $\mu\text{V/K}$), but smaller than that of PbTe (230–310 $\mu\text{V/K}$) in the same experimental conditions. The absolute Seebeck coefficients for the sample PbSe compound prepared by pressureless sintering reported in Ref. [2], showing sharper slopes with temperature, 86 $\mu\text{V/K}$ at 300 K and 266 $\mu\text{V/K}$ at 600 K.

The thermal conductivities for the studied samples $\text{PbTe}_x\text{Se}_{1-x}$ with $x=0.2, 0.3, 0.5, 0.85$ and 1.0 are shown in Fig. 4(c). The thermal conductivities for all samples prepared in this work decrease firstly and then increase slightly with increasing temperature with minimum between 450 and 600 K. The doped samples $\text{PbSe}_{1-x}\text{Te}_x$ with $x=0.2, 0.3$ and 0.5 exhibit very low thermal conductivities from 0.95 to 0.66 W/mK , which is lower than that of the pure PbTe (1.4–1.1 W/mK) in the same experimental condition from room temperature to 673 K. They are much lower than that of pure PbSe prepared by melting (2.1–1.3 W/mK) [7]. The sample with $x=0.3$ has the lowest thermal conductivity, which reaches 0.66 $\text{W m}^{-1} \text{ K}^{-1}$ at 473 K and its room-temperature thermal conductivity is 0.837 $\text{W m}^{-1} \text{ K}^{-1}$, which is comparable to the value of PbSe nanowires 0.8 $\text{W m}^{-1} \text{ K}^{-1}$ at 300 K reported by Liang et al. [8]. It is reasonable to believe that the low thermal conductivity of the samples should be originated from the enhanced phonon scattering due to the nanograins and atomic disorder between Se and Te atoms in the $\text{Pb}(\text{Se},\text{Te})$ solid solution [9]. Spark plasma sintering (SPS) technique can realize the instant sintering with short time, which can originally control the size of the grains avoiding fur-

ther coarsening. In this work, all of the samples consolidated by spark plasma sintering at 743 K for 5 min under an axial pressure of 32 MPa. The ball milling and short sintering time lead to the samples containing nanograins which certainly benefit to the reduction of the thermal conductivity.

The dimensionless figure of merit ZT for the studied samples $\text{PbTe}_x\text{Se}_{1-x}$ with $x=0.2, 0.3, 0.5, 0.85$ and 1.0 calculated by the equation $ZT = S^2 \sigma T / \kappa$ from the above data over the entire temperature range are compared in Fig. 4(d). All the doped samples exhibit higher the figures of merit than those of the pure PbTe prepared in the same condition in this work above 500 K. The sample $\text{PbTe}_x\text{Se}_{1-x}$ with $x=0.5$ shows the highest dimensionless figure of merit ZT of 1.15 at 573 K, which is higher than 0.75 of the pure PbTe at 473 K prepared in the same condition in this work, or higher than 0.8 of the pure PbTe fabricated by a combination of the hydrothermal method and hot pressing [10].

4. Conclusion

The n-type semiconductors $\text{PbTe}_x\text{Se}_{1-x}$ containing nanograins were prepared by high-frequency induction melting, ball milling and SPS techniques. Low electrical resistivities were found in the doped samples due to the modification of the interface between the grains by the formation of the solid solution $\text{Pb}(\text{Se},\text{Te})$ by diffusion of Se and Te between the PbTe and PbSe phases in the mixture powders during ball milling and SPS process. A very low thermal conductivity was attained in the doped samples $\text{PbSe}_{1-x}\text{Te}_x$ with $x=0.2, 0.3$ and 0.5 due to the nanograins and atomic disorder between Se and Te atoms in the $\text{Pb}(\text{Se},\text{Te})$ solid solution. The maximum dimensionless figure of merit ZT of 1.15 was obtained in the sample $\text{PbTe}_{0.5}\text{Se}_{0.5}$ at 573 K, more than 50% higher than that of pure PbTe prepared in the same condition.

Acknowledgments

The work was supported by the National Natural Science Foundation of China (Nos.: 50871070 and 51003060) and Shenzhen Science and Technology Research Grant (Nos.: CXB200903090012A and JC200903120109A). The authors would like to thank Ms. L.D. Zhou for her help in experiment.

References

- [1] G.T. Alekseeva, E.A. Gurieva, P.P. Konstantinov, L.V. Prokofeva, M.I. Fedorov, *Semiconductors* 30 (1996) 1125.
- [2] H. Unuma, N. Shigetsuka, M. Takahashi, *J. Mater. Sci. Lett.* 17 (1998) 1055–1057.
- [3] D. Parker, D.J. Singh, *Phys. Rev. B* 82 (2010) 035204.
- [4] M.M. Ibrahim, S.A. Saleh, E.M.M. Ibrahim, A.M. Abdel Hakeem, *J. Alloys Compd.* 452 (2008) 200.
- [5] T.C. Harman, P.J. Taylor, M.P. Walsh, B.E. La-Forge, *Science* 297 (2002) 2229–2232.
- [6] C.H. Kuo, M.S. Jeng, J.R. Ku, S.K. Wu, Y.W. Chou, C.S. Hwang, *J. Electron. Mater.* 38 (2009) 1956–1961.
- [7] A.A. El-Sharkawy, A.M. Abou El-Azm, M.I. Kenawy, A.S. Hillal, H.M. Abu-Basha, *Int. J. Thermophys.* (1983) 261–269.
- [8] W.J. Liang, O. Rabin, A.I. Hochbaum, M. Fardy, M.J. Zhang, P.D. Yang, *Nano Res.* 2 (2009) 394–399.
- [9] W. Kim, J. Zide, A. Gossard, D. Klenov, S. Stemmer, A. Shakouri, A. Majumdar, *Phys. Rev. Lett.* 96 (2006) 045901.
- [10] Y.Q. Cao, T.J. Zhu, X.B. Zhao, *J. Phys. D: Appl. Phys.* 42 (2009) 015406.